



In Vitro Characterization of a Novel C,N-cyclometalated Benzimidazole Ru(II) Arene Complex: Stability, Intracellular Distribution and Binding, Effect on Organic Osmolyte Homeostasis and Induction of Apoptosis

Journal:	<i>Metallomics</i>
Manuscript ID:	MT-ART-02-2015-000056.R1
Article Type:	Paper
Date Submitted by the Author:	13-Mar-2015
Complete List of Authors:	Dam, Celina; University of Copenhagen, Pharmacy; University of Copenhagen, Biology Pérez, Sergio; Universidad de Murcia, Química Inorganica Tsolakou, Theodosia; University of Copenhagen, Pharmacy Segato, Christian; University of Copenhagen, Biology Gammelgaard, Bente; University of Copenhagen, Department of Pharmacy Yellol, Gorakh; Universidad de Murcia, Química Inorganica Ruiz, Jose; Universidad de Murcia, Departamento de Química Inorganica Lambert, Ian; University of Copenhagen, Department of Biology, Section for Cell and Developmental Biology Stürup, Stefan; University of Copenhagen, Department of Pharmacy

***In Vitro* Characterization of a Novel C,N-cyclometalated Benzimidazole Ru(II) Arene Complex: Stability, Intracellular Distribution and Binding, Effect on Organic Osmolyte Homeostasis and Induction of Apoptosis**

Celina Støving Dam^{a,b}, Sergio Alejo Perez Henarejos^c, Theodosia Tsolakou^{a,b}, Christian Alexander Segato^b, Bente Gammelgaard^a, Gorakh S. Yellol^c, José Ruiz^c, Ian Henry Lambert^b and Stefan Stürup^a

^aUniversity of Copenhagen, Department of Pharmacy, Universitetsparken 2, 2100 Copenhagen Ø, Denmark

^bUniversity of Copenhagen, Department of Biology, Universitetsparken 13, 2100 Copenhagen Ø, Denmark

^cDepartment of Inorganic Chemistry and Regional Campus of International Excellence "Campus Mare Nostrum", University of Murcia and Institute for Bio-Health Research of Murcia IMIB-Arrixaca, E-30071 Murcia, Spain

Abstract

In the present work a novel C,N-cyclometalated benzimidazole Ru(II) arene complex (GY34) was characterized applying an alternate, diverse approach considering both chemical and biological aspects. RP-HPLC-ICP-MS and RP-HPLC-ESI-MS analysis proved that GY34 in both RPMI-1640 cell medium and ammonium acetate buffer was transformed to several subspecies and the importance of evaluating and controlling analyte stability throughout experiments was demonstrated. Applying a novel cell fractionation protocol GY34 was found to target cell nuclei and mitochondria in Ehrlich Lettré Ascites (ELA) cells, with the intracellular distribution depending on GY34 concentration in the cell medium during incubation. In ELA cells 96 ± 0.2 % of cytosolic GY34 was bound to high-molecular species. Furthermore, using tracer technique GY34 was found to reduce uptake and increase release of the organic osmolyte taurine in ELA cells, with innate resistance to Cisplatin and in A2780 human ovarian cancer cells, with acquired resistance to Cisplatin. Importantly, FACS analysis revealed that GY34 induced apoptosis in ELA cells. The present data suggest a potential of GY34 in overcoming Cisplatin resistance. The methodology applied can be used as a general protocol and an additional tool in the initial evaluation of novel metal-based drugs.

Introduction

Today cancer ranges among the principal causes of morbidity and mortality worldwide and the World Health Organization expects a 70 % increase in the number of new cases over the next two decades.¹ For many years Cisplatin has been the choice of treatment for a wide range of cancers, *e.g.* ovarian, testicular, head and neck, bladder and lung cancer.² However, the efficiency of Cisplatin is limited by acquired or intrinsic resistance³ and by severe side effects such as ototoxicity, peripheral neuropathy, myelosuppression and nephrotoxicity.⁴

Consequently, focus is shifting towards the discovery of novel improved anti-cancer drugs and numerous new compounds are synthesized in the search of a promising drug candidate. In the initial work of selecting a candidate with an ideal profile, determination of IC₅₀ values, apoptotic studies and cell cycle checkpoint assays are usually performed. However, knowledge on the stability of the compound and the mechanism of action is

also very valuable when deciding on the further fate of a new compound. Particularly, the latter is of significant importance as a mechanism of action dissimilar to that of Cisplatin may be able to overcome Cisplatin resistance, and hence improve anti-cancer therapy.

The purpose of the current work was to characterize the novel *C,N*-cyclometalated $[(\eta^6\text{-}p\text{-cym})\text{RuCl}(\kappa^2\text{-}N,C\text{-}L)]\text{L}$ = deprotonated 1-butyl-2-phenyl-benzimidazole carboxylate complex GY34 (Fig. 1, published by Yellol et al.⁵) applying a more diverse approach than usually employed, addressing both biological and chemical aspects of the compound. GY34 has been shown to exert an increased cytotoxic activity compared to Cisplatin in colorectal adenocarcinoma HT29 cells (IC_{50} GY34: $2.2 \pm 0.4 \mu\text{M}$, IC_{50} Cisplatin: $9.5 \pm 0.2 \mu\text{M}$), in human breast cancer T47D cells (IC_{50} GY34: $5.5 \pm 0.2 \mu\text{M}$, IC_{50} Cisplatin: $38 \pm 2 \mu\text{M}$) and in Cisplatin-resistant human ovarian cancer A2780 cells (IC_{50} GY34: $6.4 \pm 0.1 \mu\text{M}$, IC_{50} Cisplatin: $15 \pm 1 \mu\text{M}$).⁵ Moreover, GY34 arrests cells in the S phase of the cell cycle and induces apoptosis of HT29 cells.⁵ Finally, the level of metal accumulation in T47D cells was increased after treatment with GY34 relative to treatment with Cisplatin.⁵ Altogether this presents GY34 as a potential future drug candidate for anti-cancer treatment and signifies the importance of further investigation of the compound.

Experimental

Reagents

All reagents were analytical grade and purchased from Sigma-Aldrich (St. Louis, MO, USA) unless otherwise stated.

The Ru-based compound GY34 was synthesized as described elsewhere⁵ in the research group of Prof. José Ruiz, Department of Inorganic Chemistry, University of Murcia, Spain. 1 mM stock solutions of GY34 were prepared in DMSO. For cell experiments volumes of 1 mM GY34 stock solutions in DMSO were added directly to the cell medium to obtain the preferred concentration. GY34 concentrations applied in the various experiments were selected on the basis of the IC_{50} value for human ovarian cancer A2780 cells reported by Yellol et al.⁵ (refer to Introduction). The applied concentration of Cisplatin was based on previously performed caspase 3 activity assay.⁶

The mobile phase for RP-HPLC-ICP-MS and RP-HPLC-ESI-MS analysis consisted of 20 mM ammonium acetate in 65 % v/v MeOH, pH 6.8.

PBS for cell culturing and cell fractionation consisted of 137 mM NaCl, 2.6 mM KCl, 6.5 mM Na_2HPO_4 and 1.5 mM KH_2PO_4 , pH 7.4. KCl-Tris buffer used for cell fractionation consisted of 100 mM KCl, 50 mM Tris-HCl, 5 mM MgCl_2 , 1 mM Na_2EDTA , pH 7.4. Lysis buffer consisted of 1 % SDS, 150 mM NaCl, 20 mM HEPES, 1 mM EDTA, 0.5 % Triton X-100, 1 mM NaVO_3 and 1 % protease inhibitor. Percoll (GE Healthcare, Wauwatosa, WI, USA) solutions were prepared in KCl-tris buffer. The isotonic NaCl medium and MgCl_2 solution used for taurine flux experiments contained 143 mM NaCl, 5 mM KCl, 1 mM Na_2HPO_4 , 1 mM CaCl_2 , 1 mM MgSO_4 , 10 mM HEPES and 100 mM MgCl_2 , respectively.

1
2
3
4
5
6
7
8
9
10
11
12
13
14
15
16
17
18
19
20
21
22
23
24
25
26
27
28
29
30
31
32
33
34
35
36
37
38
39
40
41
42
43
44
45
46
47
48
49
50
51
52
53
54
55
56
57
58
59
60

80

SDS page gel electrophoresis and western blotting were performed using materials from Invitrogen Life Technologies (Thermo Fischer Scientific, Waltham, MA, USA): XCell SureLock Mini-Cell, 1.0 mm 10 well NuPAGE Novex 10 % Bis-Tris gels, NuPAGE LDS Sample Buffer, BenchMark Protein Ladder, NuPAGE MOPS SDS Running Buffer, NuPAGE Antioxidant, XCell II Blot Module, 0.2 μm Nitrocellulose Pre-Cut Blotting Membranes and NuPAGE Transfer Buffer. Membranes were blocked with 5 % non-fat dry milk (retail store) in TBST, *i.e.* 0.01 M Tris-HCl, 0.15 M NaCl, 0.1 % tween 20, pH 7.4. Primary rabbit mAb antibodies against histone H3 (1:500, 18 kDa, Cell Signaling Technology, Danvers, MA, USA), malate dehydrogenase 2 (1:100, 36 kDa) and lactate dehydrogenase B (1:1000, 35 kDa, Novus Biologicals, Littleton, CO, USA) were used along with secondary anti-rabbit IgG antibody (1:5000). Bands were developed using BCIP/NBT Phosphatase Substrate 3-component System (Kirkegaard & Perry Laboratories Inc., Gaithersburg, MD, USA).

The Ru standard used for the ICP-MS determinations was purchased from CPI International (Santa Rosa, CA, USA) and was a custom made multi-element standard containing Au, Ir, Pd, Pt, Os and Rh apart from Ru. The standards for external calibration were prepared in a diluted acid solution containing 0.1 % HCl and 0.65 % HNO_3 . The same mixture of diluted acids was used to dilute samples for ICP-MS analysis.

The incubation buffer used for the apoptosis assay consisted of 10 mM HEPES, 140 mM NaCl and 5 mM CaCl_2 , pH = 7.4. The labeling solution was prepared by diluting 20 μL annexin-V-Fluos labeling reagent (Roche, Basel, Switzerland) in 1 mL incubation buffer and adding 20 μL 50 $\mu\text{g}/\text{mL}$ propidium iodide solution.

Stability of GY34 in cell medium and mobile phase

The stability of GY34 in dilute solution was initially examined by RP-HPLC-ICP-MS analysis applying an Agilent 1100 Series HPLC system consisting of a quaternary pump, a degasser and an autosampler (Agilent Technologies, Santa Clara, CA, USA). HPLC was performed using a Phenomenex (Torrance, CA, USA) Luna C18 column (3 μm , 100 \AA , 100 x 2 mm), flow rate 200 $\mu\text{L}/\text{min}$ and an injection volume of 20 μL . The HPLC system was connected to a Perkin Elmer (Waltham, MA, USA) Sciex ELAN 6100 DRC-e ICP-MS instrument via a Cetac (Teledyne Technologies Inc., Omaha, NE, USA) Aridus II membrane desolvation system in order to remove organic solvent from the mobile phase prior to introduction into the ICP-MS instrument (refer to Møller et al.⁷ for thorough description of setup). The desolvation system was equipped with a Cetac 200 $\mu\text{L}/\text{min}$ C-flow PFA concentric nebulizer, spray chamber temperature was 110 $^\circ\text{C}$, desolvator temperature was 160 $^\circ\text{C}$, argon sweep gas flow was 5 L/min and nitrogen gas flow was 6 mL/min. The ICP-MS dwell time was 200 ms and 1 sweep/reading, 1 replicate and 500 readings/replicate were applied. Isotopes $^{99}\text{Ru}^+$ and $^{101}\text{Ru}^+$ were monitored. Nebulizer gas flow was 0.9 mL/min while RF power and lens voltage were optimized on a daily basis. A 10 ppb Ru standard prepared in 0.1 % HCl and 0.65 % HNO_3 yielded a signal of ~ 142000 counts. 1 μM solutions of GY34 (corresponding to 100 ppb Ru) in mobile phase and Roswell Park Memorial Institute (RPMI-1640) cell medium, respectively, were analyzed immediately after preparation and after 24 h at room temperature.

In order to elucidate the structure of the various GY34 species indicated by the RP-HPLC-ICP-MS analysis RP-HPLC-ESI-MS was performed using the same HPLC system and parameters as described above, but with a

1
2
3
4
5
6
7 120 manual injector and with an injection volume of 5 μL . The HPLC system was connected to a Bruker (Billerica,
8 121 MA, USA) Esquire ion trap equipped with an electrospray ionization source. ESI-MS was performed using the
9 122 following parameters: Positive ionization mode, 300-2200 m/z scan window, 50 ms max. accumulation time,
10 123 50000 ion charge control target, average 5, 10 L/min drying gas flow, 350 °C drying gas temperature, 45 psi
11 124 nebulizer gas, 214 V RF amplitude, 42 trap drive, 53 V capillary exit, 18 V skimmer 1, 5.7 V skimmer 2. A 1 mM
12 125 GY34 solution prepared in DMSO and RPMI-1640 cell medium (20:80 % v/v) was analyzed immediately after
13 126 preparation and after 24 h incubation at room temperature.
14 127

15 128 **Cell culturing**

16 129 Murine Ehrlich Lettré Ascites (ELA) cells, an adherent subtype of the non-adherent wild type Ehrlich Ascites
17 130 Tumor cells (EATCs), were obtained from ATCC (Washington, DC, USA) and grown in RPMI-1640 cell medium
18 131 supplied with 10 % heat-inactivated fetal bovine serum and 1 % antibiotics (penicillin, streptomycin). The cells
19 132 were kept as a monolayer in 75 cm² CellStar culture flasks at 37 °C, 5 % CO₂, 100 % humidity and passaged
20 133 every 3-4 days using 0.5 % trypsin in PBS to detach cells.
21 134

22 135 A2780 human ovarian carcinoma Cisplatin-sensitive wild-type (A2780 WT, provided by Dr. Antonio Donaire,
23 136 University of Murcia, Spain) and Cisplatin-resistant (A2780 RES, kindly donated by Dr. Isolda Romero-Canelón,
24 137 University of Warwick, United Kingdom) cells were grown and passaged at similar conditions, however with 1 %
25 138 L-glutamine added to the cell medium. Cisplatin resistance in A2780 RES cells was maintained by treatment
26 139 with 1 μM Cisplatin between every third passages.
27 140

28 141 **Cell fractionation**

29 142 Prior to fractionation ELA cells were grown to 80-90 % confluence in four 175 cm² culture flasks at 37 °C, 5 %
30 143 CO₂, 100 % humidity and incubated at the same conditions for 18 h with a nominal concentration of 10 μM
31 144 GY34. Immediately before the fractionation was initiated a sample of the cell medium was taken out in order to
32 145 measure the GY34 concentration in the medium and evaluate stability and solubility of the compound. An
33 146 overview of the cell fractionation procedure appears from Fig. 2. The fractionation was performed at room
34 147 temperature; however in between each step in the process samples were kept on ice in order to minimize
35 148 degradation. The roman numbers in the following provide overview of the different fractionation steps and
36 149 should be related to Fig. 2.
37 150

38 151 (i) Initially, the cell medium was removed and the cells in each of the four 175 cm² culture flasks were washed
39 152 in 5 mL PBS. The PBS was removed, 5 mL 0.5 % trypsin in PBS was added and the cells were left at 37 °C until
40 153 loosened. The cells were then resuspended in 10 mL RPMI-1640 medium and the cell suspensions in the four
41 154 175 cm² culture flasks were transferred to four falcon tubes. The cells were washed twice in 5 mL PBS
42 155 (centrifuging 4 min/500 G) and pooled in two falcon tubes. After removing the PBS 1 mL KCl-tris buffer was
43 156 added to each falcon tube. KCl-tris buffer was used to mimic cellular ion composition. The cells were
44 157 resuspended and the cell suspension in each falcon tube was transferred to an eppendorf tube. From each
45 158 tube 50 μL cell suspension (unbroken cells) was collected. The remaining of the cell suspensions were then
46 159 centrifuged (1 min/1200 G/4 °C) and the supernatants discarded. The remaining pellets (unbroken cells) were
47
48
49
50
51
52
53
54
55
56
57
58
59
60

1
2
3
4
5
6
7
8
9
10
11
12
13
14
15
16
17
18
19
20
21
22
23
24
25
26
27
28
29
30
31
32
33
34
35
36
37
38
39
40
41
42
43
44
45
46
47
48
49
50
51
52
53
54
55
56
57
58
59
60

each resuspended in 100 μ L KCl-tris buffer. (ii) The cells were homogenized using polypropylene pellet pestles (2 x 10 strokes, put on ice in between) and 700 μ L KCl-tris buffer was added to each eppendorf tube. (iii) The homogenized cells were centrifuged (1 min/1200 G/4 $^{\circ}$ C) and (iv) 700 μ L of each of the supernatants (mitochondria and cytosol) were collected in new eppendorf tubes. (vii) The remaining pellets (crude nuclei) were stored on ice for later purification. (v) The collected supernatants were centrifuged (5 min/1500 G/4 $^{\circ}$ C), (vi) the resulting supernatants pooled and the pellet discarded. (vii) The pooled supernatant was centrifuged (10 min/9000 G/4 $^{\circ}$ C) and (viii) the resulting supernatant (**cytosolic fraction**) collected. To 93 μ L of the cytosol fraction 5 μ L 10 % SDS, 1 μ L NaVO₃ and 1 μ L protease inhibitor were added; this was used for protein determination and western blotting. (ix) The remaining pellet (crude mitochondria) (x) was washed three times in 500 μ L KCl-tris buffer (centrifuging 10 min/9000 G/4 $^{\circ}$ C) and (xi) the pellet (mitochondria) was collected and resuspended in 70 μ L lysis buffer (**mitochondrial fraction**).

(xiii) The crude nuclei were each resuspended in 600 μ L 24 % percoll and each 24 % suspension was carefully placed on top of 1 mL 40 % percoll in new eppendorf tubes creating two layers. The two-layer suspensions were centrifuged (10 min/15000 G/4 $^{\circ}$ C) causing the nuclei to migrate through the 24 % percoll layer to the bottom of the 40 % percoll layer and leaving impurities in the 24 % percoll layer. For each centrifuged two-layer suspension most of the upper phase was removed and (xiv) 300 μ L of the nuclei band (semi-crude nuclei) was collected and resuspended in 1 mL KCl-tris buffer followed by centrifugation (10 min/15000 G/4 $^{\circ}$ C). (xv) The pellets were each washed in 500 μ L KCl-tris buffer, centrifuged (10 min/15000 G/4 $^{\circ}$ C) and pooled. The pooled pellet was washed in 500 μ L KCl-tris buffer, centrifuged (10 min/15000 G/4 $^{\circ}$ C) and (xvi) the resulting pellet (nuclei) resuspended in 100 μ L lysis buffer (**nuclear fraction**) and sonicated.

Three replicates of the fractionation were made; *i.e.* cells from three different passages of the ELA cells were fractionated.

Protein determination

Protein content in cell fractions, used for SDS page gel electrophoresis, was determined by a Bradford colorimetric assay (Bio-Rad, Hercules, CA), measuring absorbance at 600 nm (GeneQuant Pro spectrophotometer, GE Healthcare) and correlating values to a standard curve (0-30 μ g/ μ L). Protein content in influx experiments was determined by a standard Lowry method using standards in the range 0-1 mg/mL.

Evaluation of cell fractionation

The purity of the cell fractions was evaluated by western blotting. Samples containing the same amount of protein (15–20 μ g) were proceeded for SDS page gel electrophoresis together with a crude total cell homogenate as control. Protein was then transferred to nitrocellulose membranes and the transfer was confirmed by Ponceau staining. The membranes were blocked for 1 h at 37 $^{\circ}$ C, incubated with primary antibody in a humid chamber over night at 4 $^{\circ}$ C and washed with TBST. The membranes were then incubated in a humid chamber with secondary antibody for 1 hour at room temperature, washed with TBST and developed using BCIP/NBT Phosphatase Substrate.

Quantitation of GY34

For quantitation of GY34 a Perkin Elmer Sciex Elan 6000 ICP-MS instrument, equipped with a Perkin Elmer low-flow GemCone nebulizer and a Glass Expansion (West Melbourne Vic, Australia) cyclonic spray chamber, was applied. RF power, lens voltage and nebulizer gas flow were optimized on a daily basis. The remaining instrumental parameters applied were: 45 s sample flush, 30 s read delay, 90 s wash, 1 sweep/reading, 25 readings/replicate, 5 replicates, 50 ms dwell time and isotopes $^{99}\text{Ru}^+$ and $^{101}\text{Ru}^+$ were monitored. Samples were delivered to the ICP-MS instrument with the aid of a Cetac ASX-110FR autosampler. Prior to analysis samples were prepared according to the following: Exact volumes were evaporated to dryness using an Eppendorf (Hamburg, Germany) Concentrator Plus vacuum centrifuge. Subsequently, samples (excl. nuclei) were digested on a heat block with 200 μL 65 % HNO_3 and 50 μL 30 % H_2O_2 at 60 $^\circ\text{C}$ for 6 h while nuclei were digested in a CEM (Matthews, NC, USA) MDS-81D microwave oven with 400 μL 65 % HNO_3 and 100 μL 30 % H_2O_2 for 10 min at 60 % capacity (corresponds to approximately 10 W). The digests were diluted to 5 mL, filtered (Q-max[®] RR Syringe Filters, 0.45 μm , Frisette, Knebel, Denmark) and further diluted before analysis, if necessary. The cell medium was not digested, but diluted 200 times and filtered before analysis. The GY34 concentration was determined by external calibration (0-10 ppb Ru). LOD = 0.005 ppb (blank + 3*SD of blank).

Binding of GY34 to cytosolic biomolecules

The distribution of GY34 between high- and low-molecular species in the cytosol was studied using centrifugal filtration. ELA cells were grown to 80-90 % confluence in a 175 cm^2 culture flask at 37 $^\circ\text{C}$, 5 % CO_2 , 100 % humidity and were then incubated with 10 μM GY34 for 18 h at the same conditions. The cytosol was isolated by the following procedure: After removing the cell medium the cells were washed twice in 10 mL PBS and the PBS was removed. 250 μL lysis buffer was added, the cells were collected using a rubber policeman, sonicated and centrifuged (5 min/20000 G/4 $^\circ\text{C}$). The resulting supernatant (cytosol) was collected. An exact volume of the cytosol was then fractionated using 3 kDa Amicon Ultra 2 mL spin filters (EMD Millipore, Billerica, MA, USA). The cytosol was centrifuged (60 min/4500 G/4 $^\circ\text{C}$) and the filtrate (<3 kDa fraction) was collected. The filter was reversed, centrifuged (15 min/1500 G/4 $^\circ\text{C}$) and the concentrate (>3 kDa fraction) was collected. The content of GY34 in the <3 kDa and >3 kDa fractions and the unfractionated cytosol was determined as described above. The experiment was performed *in triplo*, i.e. on three different passages of ELA cells.

Taurine flux assays

Taurine uptake via the taurine transporter (TauT) as well as taurine release under isotonic conditions from A2780 WT, A2780 RES and ELA cells grown in the presence of either 5 μM Cisplatin or 5 μM GY34 for 18 h were determined by tracer technique at room temperature as previously described.^{8,9} For influx experiments cells were grown to 80 % confluence in 6-well polyethylene culture plates (9.6 cm^2 per well). Five wells were used to determine the taurine uptake and the residual well was used to determine the representative protein content in a well. Cells were washed three times with isotonic NaCl medium and left with 600 μL isotonic NaCl medium. Influx was initiated by addition of 50 μL ^3H -taurine stock solution containing 37000 Bq/mL (0.005 μM taurine) to well 1-5 at time 0, 2, 4, 6 and 8 min. Influx was terminated by removal of the extracellular medium at time 10 min, rapid rinse of cells by addition/aspiration of 1 mL ice-cold MgCl_2 solution, followed by cell lysis with 96 % ethanol. After evaporation of ethanol, ^3H -activity was extracted with ddH_2O and determined in a Perkin

1
2
3
4
5
6
7 240 Elmer scintillation counter using Ultima Gold™. The cellular taurine content (nmol·g protein⁻¹) in each well was
8 241 determined from the ³H-aurine activity (cpm·well⁻¹) using the extracellular specific activity (cpm·nmol⁻¹) and
9 242 the protein content (mg protein·well⁻¹). Taurine uptake (nmol·g·protein⁻¹·min⁻¹) was determined as the slope of
10 243 a plot of cellular taurine content plotted versus time using linear regression. At least three replicates of the
11 244 experiment were made, *i.e.* on three different passages of each of the three cell lines.
12 245

13 246 Taurine efflux was estimated on cells grown to 80 % confluence in 6-well polyethylene culture plates and
14 247 loaded in cell media supplemented with ³H-aurine (18500 Bq/well) for 2 h (37 °C, 5 % CO₂, 100 % humidity).
15 248 Before initiation of the efflux the loading medium and the cells were washed three times with 1 mL isotonic
16 249 NaCl medium. The efflux experiment was performed by transferring the NaCl medium from the well to vials
17 250 and replacing it with new medium at two minute intervals. After removal of the last sample, isotope remaining
18 251 inside the cells was determined by addition of 1 mL 1 M NaOH, gently shaking (1 h) and subsequently transfer
19 252 of NaOH and to times wash-outs (ddH₂O) to vials. ³H-activity was determined using Ultima Gold™. The total ³H
20 253 activity in the cell system was determined as the sum of ³H activity released during the efflux experiment and
21 254 ³H activity detected in the NaOH/ddH₂O wash-outs. The fractional rate constant (min⁻¹) for taurine release
22 255 under isotonic conditions was calculated from the equation: $k = \frac{\ln(X_1) - \ln(X_2)}{t_1 - t_2}$ where X₁ and X₂ are the fractions
23 256 remaining in the cell at time t₁ and t₂, divided by the time interval. At least three replicates of the experiment
24 257 were made, *i.e.* on three different passages of each of the three cell lines.
25 258

26 259 **Apoptosis assay**

27 260 Apoptosis studies on cells exposed to Cisplatin and GY34 were performed by flow cytometry. 10⁵ ELA cells were
28 261 seeded in 2 mL RPMI-1640 cell medium in 6-well plates and incubated for 24 h at 37 °C, 5 % CO₂. Cells were
29 262 subsequently exposed to 5 μM GY34 or 5 μM Cisplatin for 18 h under the same conditions. One well remained
30 263 untreated serving as a control. After incubation the cell medium was collected and the cells detached by
31 264 trypsination (0.25 % trypsin/0.5 mM EDTA in 1 mL PBS, 37 °C, 3 min). Trypsin was inactivated by addition of 1
32 265 mL cell medium. The resulting 2 mL cell suspension was added to the collected cell medium hence permitting
33 266 both floating and adherent cells to be considered in the assay. The cells were centrifuged (10 min/250 G) and
34 267 the precipitated cells washed twice in 1 mL PBS. PBS was removed after the final centrifugation and cells were
35 268 resuspended in 160 μL incubation buffer. Subsequently, 40 μL of labeling solution was added and the cells were
36 269 protected from light at room temperature for 15 min. 200 μL PBS was added immediately before detection of
37 270 light emission at wavelengths of 620 nm (propidium iodide) and 525 nm (annexin-V) using a Becton-Dickinson
38 271 FACSCalibur flow cytometer (BD Biosciences, San Jose, CA, USA). During registration 10000 events were
39 272 acquired in each case. The experiment was performed *in duplo*, *i.e.* on two different passages of ELA cells.
40 273

41 274 **Results and discussion**

42 275 In this work the novel Ru-based complex GY34 (Fig. 1) was characterized with respect to stability and
43 276 transformation in solution, intracellular distribution and binding to cytosolic biomolecules, organic osmolyte
44 277 flux across cells along with its ability to induce apoptosis. Relevant comparisons to Cisplatin were made.
45 278

Stability of GY34 in cell medium and mobile phase

The stability of GY34 in dilute solution was evaluated applying RP-HPLC-ICP-MS analysis. 1 μ M solutions of GY34 in mobile phase (20 mM ammonium acetate in 65 % v/v MeOH, pH 6.8) and RPMI-1640 cell medium, respectively, were analyzed immediately after preparation and after 24 h at room temperature. The results are outlined in Fig. 3. The chromatograms obtained immediately after preparation of the GY34 solutions both contain one large peak (t_r \sim 4.5 min) that most likely can be assigned to GY34. After 24 h at room temperature a second large peak (t_r \sim 2 min) appears. This indicates that GY34 at room temperature is transformed to another Ru-containing species and that the transformation occurs in both mobile phase and cell medium.

The structures of the GY34 species were attempted elucidated by RP-HPLC-ESI-MS. A 1 mM GY34 solution prepared in DMSO and RPMI-1640 cell medium (20:80 % v/v) was analyzed immediately after preparation (total ion chromatogram (TIC) displays one large peak at t_r \sim 4.5 min and a smaller peak at t_r \sim 2 min, not shown) and after 24 h at room temperature (Fig. 4 and 5). Taking into account the slight difference in retention time caused by different dead volumes in the RP-HPLC-ICP-MS and RP-HPLC-ESI-MS systems the three peaks seen in Fig. 4 most likely correspond to the peaks at t_r \sim 2, \sim 3 and \sim 4.5 min in the ICP-MS chromatograms in Fig. 3. The dissimilar peak intensity between the ICP-MS and ESI-MS chromatograms is probably due to the different sensitivity of the two methods. The respective mass spectra (Fig. 5) prove that the \sim 3 min TIC peak contains species of m/z 529.3 and 607.2 and that the \sim 4.5 min TIC peak corresponds to species of m/z 543.2 and 621.3. Verified by comparison to the theoretical mass spectrum (refer to Supplementary material) the \sim 3 min TIC peak can be assigned to the structure of GY34 where chloride is removed and the methyl ester is hydrolyzed (m/z 529.3, refer to Fig. 5 for structure) and to the same structure with DMSO added (m/z 607.2). In the same manner the \sim 4.5 min TIC peak can be assigned to GY34 without the chloride (m/z 543.2, refer to Fig. 5 for structure) and to the same structure with DMSO added (m/z 621.3). The addition of DMSO to the GY34 species is not expected to occur in solution but rather as a result of an interaction between GY34 and DMSO in the ESI-MS interface. The mass spectrum of the \sim 2 min TIC peak (not shown) did not allow for structure elucidation of the related Ru species as the characteristic Ru isotopic pattern was absent. An explanation could be that the \sim 2 min TIC peak corresponds to a GY34 subspecies that is fragmented during ESI leaving the Ru-containing fragment unionized and hence not detectable by ESI-MS, but still able to produce a signal in ICP-MS as it contains Ru.

Figure 5 demonstrates that the chloride of GY34 is removed immediately after dissolving the compound in cell medium or mobile phase. In addition to this GY34 is transformed to several different species as a function of time. Thus the cytotoxic activity of GY34 proposed by Yellol et al.⁵ is most likely not caused by GY34 itself but instead by a subspecies of the compound. This is in accordance with the knowledge that Cisplatin as well in solution is hydrolyzed, exchanging one or both chlorides with water.¹⁰ The possible transformation in solution of newly synthesized metallo-drugs should therefore be kept in mind when performing experiments.

Another important aspect of stability in solution is the solubility of the analyte. By NMR it has been shown that GY34 is soluble in pure DMSO at 20 mM concentration, and that 200 μ M GY34 solutions prepared in 10 % DMSO are stable in up to 48 h.¹¹ Slightly soluble compounds often precipitate over time and the actual

1
2
3
4
5
6
7
8
9
10
11
12
13
14
15
16
17
18
19
20
21
22
23
24
25
26
27
28
29
30
31
32
33
34
35
36
37
38
39
40
41
42
43
44
45
46
47
48
49
50
51
52
53
54
55
56
57
58
59
60

concentration applied when performing experiments may not be consistent with the expected concentration. In the current work the intracellular distribution of GY34 was investigated as described below. For these experiments GY34 was added to the cell medium to obtain a nominal concentration of 10 μM . After incubation an aliquot of the cell medium was taken out and the GY34 concentration was determined by ICP-MS analysis. Interestingly, actual GY34 concentrations in the cell medium were found to range between $\sim 2\text{-}10$ μM for different replicates. As discussed below the intracellular distribution of GY34 appears to be dependent on the GY34 concentration in the cell medium during incubation. Once more, this establishes analyte stability as a very critical parameter and stresses the significance of evaluating and controlling the actual analyte concentration throughout experiments.

The limited solubility of GY34 in the cell medium also signifies the importance of the procedure used to prepare samples for ICP-MS analysis. Simply filtering and diluting the samples will cause potentially precipitated GY34 to be lost and lead to erroneous results. In this work the samples were digested at 60 $^{\circ}\text{C}$ using 65 % HNO_3 and 30 % H_2O_2 , with nuclei even requiring microwave digestion. Thus, should some GY34 precipitate in the samples prior to ICP-MS determination the result will not be affected as the sample preparation procedure will cause all GY34 to be dissolved.

Intracellular distribution of GY34

In order to obtain knowledge on the mechanism of action of GY34 the intracellular distribution of the compound in ELA cells was investigated. The cells were incubated for 18 h with nominally 10 μM GY34 and afterwards the cell suspension was fractionated to a nuclear, a mitochondrial and a cytosolic fraction applying a novel protocol developed for this work (refer to Fig. 2 and the experimental section Cell Fractionation). The content of GY34 in each fraction was determined by ICP-MS analysis and the result appears from Table 1. According to Table 1 most of the GY34 taken up by the ELA cells is located in the cytosol and the mitochondria. This indicates that GY34 might target mitochondria in contrast to Cisplatin which is known to target DNA in the cell nucleus.¹² ELA cells are known to be resistant to Cisplatin⁶ and the ability of GY34 to induce apoptosis in ELA cells (see below) might therefore arise from a different mechanism of action of GY34 compared to that of Cisplatin.

As mentioned above, the concentration of GY34 in the cell medium during incubation varied between replicates. Interestingly, the concentration in the cell medium appeared to affect the intracellular distribution on GY34. For replicate 2-3 (~ 10 μM GY34 detected in cell medium) more GY34 was located in the mitochondria compared to the nuclei (Table 1), on the other hand for replicate 1 (~ 2 μM GY34 detected in cell medium) 32 %, 10 % and 58 % of GY34 taken up by the cells were located in nuclei, mitochondria and cytosol, respectively. This indicates that GY34 at low concentrations is distributed primarily to the cell nuclei whereas the compound in higher concentrations also targets the mitochondria. Possibly, GY34 targets the cell nuclei until saturation is obtained, after which GY34 distribution to the mitochondria is initiated. It should be noted that the differing intracellular GY34 distribution between replicates is not owing to the applied cell fractionation procedure but rather related to the stability difficulties of GY34 in the cell medium. Applying the method on A2780 WT cells

1
2
3
4
5
6
7 358 incubated with 10 μ M Cisplatin yielded 1 ± 0.3 % Cisplatin in the nuclei, 6 ± 0.9 % in the mitochondria and $93 \pm$
8 359 0.6 % in the cytosol ($n = 3$), demonstrating a satisfying reproducibility between replicates.

9 360
10 361 The importance of obtaining clean fractions when predicting the intracellular distribution of a compound is
11 362 stressed by the elevated content of GY34 in cytosol compared to nuclei and mitochondria. Should the nuclei or
12 363 mitochondria be contaminated with cytosol a misleadingly higher nuclear or mitochondrial content of GY34
13 364 would appear leading to false deductions on the mechanism of action. In this work SDS page and western
14 365 blotting were performed to evaluate the purity of the obtained fractions. The result appears from Fig. 6.
15 366 Consulting Fig. 6 it can be seen that the nuclei as expected contain histone H3 (HIST, marker for nuclei) but do
16 367 not contain malate dehydrogenase 2 (MDH, marker for mitochondria) or lactate dehydrogenase B (LDH, marker
17 368 for cytosol). Thus, the nuclear fraction is not contaminated with either mitochondria or cytosol. In the same
18 369 manner the cytosol contain LDH but not HIST or MDH and the cytosol fraction is therefore not contaminated
19 370 with histone or mitochondria. The mitochondria contain a substantial amount of MDH and no HIST however a
20 371 very faded band for LDH is visible. This could indicate a minor contamination of the mitochondrial fraction with
21 372 cytosol. Conversely, the observed LDH in the mitochondria could also very likely originate from LDH embedded
22 373 in the inner mitochondrial membrane¹³ and would thus not be due to contamination with cytosol. Repeated
23 374 wash of the mitochondria (refer to step (x) in Fig. 2 and the experimental section Cell Fractionation) ought to
24 375 have removed most of the cytosol from the surface of the mitochondria. Still, it cannot be ruled out that a
25 376 small amount of cytosol has diffused into the inner membrane space of the mitochondria causing a minor
26 377 contamination. Based on the above the authors believe that the purity of mitochondrial fractions obtained
27 378 using the current fractionation protocol is sufficient and that a minor content of cytosol in the inner
28 379 mitochondrial membrane is insignificant.

29 380
30 381 Several examples of subcellular fractionation and isolation of subcellular organelles are described in the
31 382 literature.¹⁴⁻¹⁸ However, to the knowledge of the authors no procedures with features identical to the current
32 383 presented fractionation method have been reported. In the work of Hornig-Do et al. superparamagnetic
33 384 microbeads were used to isolate mitochondria from human 293 HEK, HeLa and osteosarcoma cells. Western
34 385 blotting rebutted cytosolic contamination but showed a trace of nuclei in the mitochondrial fraction. Only
35 386 mitochondria were isolated, not nuclei or cytosol.¹⁴ Applying gradient centrifugation with percoll Wieckowski
36 387 et al. were able to obtain a mitochondrial fraction from MEF cells that did not contain cytosol or nuclei.¹⁵ In the
37 388 same manner, differential centrifugation allowed Dai et al. to isolate clean mitochondria from SKOV3 and
38 389 A2780 cells.¹⁶ Neither Wieckowski et al. nor Dai et al. isolated nuclei or cytosol.^{15,16} Zayed et al. fractionated
39 390 A549 human lung adenocarcinoma epithelial cells and human HT29 and HCA7 colorectal cancer cells into
40 391 cytosol, cell membranes, nuclei and cytoskeleton using the Merck Millipore ProteoExtract® Subcellular
41 392 Proteome Extraction Kit, but did not verify the purity of the obtained fractions.¹⁷ Various fractionation kits are
42 393 commercially available however these are expensive and yield crude preparations that might need further
43 394 purification.^{19,20} In the work of Groessl et al. the Thermo Scientific Mitochondria Isolation Kit for Cultured Cells
44 395 and the Biovision FractionPREP™ Cell Fractionation Kit were used to isolate nuclei, mitochondria and cytosol
45 396 *i.a.* from A2780 cells. The western blots provided in the supplementary section of the paper show that the
46 397 mitochondria contain LDH.¹⁸ Whether this is caused by a cytosolic contamination of the mitochondria or by

1
2
3
4
5
6
7
8
9
10
11
12
13
14
15
16
17
18
19
20
21
22
23
24
25
26
27
28
29
30
31
32
33
34
35
36
37
38
39
40
41
42
43
44
45
46
47
48
49
50
51
52
53
54
55
56
57
58
59
60

LDH located in the inner mitochondrial membrane¹³ as discussed above remains unsettled. The nuclear and cytosolic fractions are clean.¹⁸ In order to map the intercellular distribution of a compound obtaining clean fractions is of high importance. Also, the method must be able to fraction cells into nuclei, mitochondria and cytosol. The authors believe that the fractionation method presented in this work features both. In addition the method is less expensive than the commercially available fractionation kits.

A critical step in the fractionation procedure is the homogenization (step (ii), Fig. 2). Applying too much force will break the mitochondria resulting in a reduced yield of mitochondria along with mitochondrial contamination of the cytosol. Conversely, when too little a force is applied, only a minor part of the cells will be homogenized. This results in a decreased mitochondrial yield as well and will furthermore contribute to the contamination of the nuclei with unbroken cells. Step (iii) in the fractionation procedure serves to precipitate the nuclei which subsequently can be removed. However, should the homogenate contain small, unbroken cells with a density similar to nuclei the nuclear fraction will be contaminated with unbroken cells and western blot bands for LDH and MDH will appear. The probability of nuclear contamination with small, unbroken cells increases with the number of unbroken cells that again depends on the force applied during homogenization. To validate the quality of the homogenization SDS page gel electrophoresis and western blotting should always be performed in connection with a fractionation.

In order to evaluate the amount of GY34 lost during the fractionation the mass balance was calculated. Prior to homogenization a volume of unbroken cells was sampled allowing the total amount of GY34 taken up by the cells to be determined by ICP-MS analysis. The mass balance was then obtained by relating the sum of the GY34 detected in the nuclear, mitochondrial and cytosolic fractions to the total GY34 taken up by the cells. $31 \pm 9 \%$ (average \pm SD, $n = 3$) of the total GY34 taken up by the cells was recovered in the fractions. A portion of GY34 was probably lost with the unbroken cells and some degree of loss is to be expected from the numerous wash and decant steps in the procedure. Finally, the effort to avoid contamination of the fractions also causes a loss: *e.g.* when decanting a supernatant a part of the supernatant had to be left on top of the pellet to ensure no pellet was transmitted. Thus, a trade-off between fraction purity and metal recovery must be made. Although a relatively small amount of GY34 was recovered in the fractions the authors do not believe that it effects the obtained distribution of GY34 in the cells. In the work of Zayed et al. mentioned above a platinum recovery of $>99 \%$ was obtained after subcellular fractionation carried out using an extraction kit.¹⁷ Apparently, the attained fractions were not washed to the same extent as the current fractionation method requires, which most likely explains the improved recovery. In this work fraction purity was prioritized due to its significance when determining the intracellular distribution, as discussed earlier.

Binding of GY34 to cytosolic biomolecules

Another way to gain knowledge on the mechanism of action of a new compound is to study whether it binds to biomolecules in the cell. As reviewed by de Almeida et al.²¹ and Casini & Reedijk²² there is every indication that the biodistribution, uptake and pharmacological action of metallo-drugs depend on interactions with proteins. In this work ELA cells were incubated with $10 \mu\text{M}$ GY34 for 18 h and the cytosol was isolated and fractionated by 3 kDa spin filters. The GY34 content in the resulting two fractions was determined by ICP-MS analysis. $96 \pm$

1
2
3
4
5
6
7 438 0.2 % (average \pm SD, n = 3) of the GY34 in the cytosol was found in the high-molecular fraction (>3 kDa). This
8 indicates that in the cytosol the majority of GY34 is bound to high-molecular biomolecules, most likely proteins,
9 439 and that only a minor part of the compound remains unbound or bound to small molecules. Thus the
10 440 cytotoxicity of GY34 is most likely facilitated by interaction with protein targets.
11 441
12 442

13 443 Similar experiments were carried out by Kasherman et al. with Cisplatin on A2780 cells suggesting that two-
14 444 thirds of Cisplatin was associated with >3 kDa species.²³ This supports the hypothesis that metallo-drugs bind to
15 445 proteins once inside the cytosol instead of remaining unbound. The hypothesis is to some extent supported by
16 446 the work of Heffeter et al. Performing SEC-ICP-MS on cytosol of human cervical carcinoma-derived KB-3-1 cells
17 447 treated with the Ru-based drug KP1019 and its sodium salt KP1339 they found that after 3 h the majority of Ru
18 448 was found in the >150 kDa fraction and that Ru was redistributed to the <40 kDa fraction after 24 h.²⁴
19 449
20 449
21 449
22 449

23 450 In order to validate that no GY34 was lost in the spin filters the GY34 content in the unfractionated cytosol was
24 451 determined as well, allowing calculation of the mass balance. 91 ± 9 % (average \pm SD, n = 3) of the total
25 452 cytosolic GY34 was located in the <3 kDa and >3 kDa fractions validating an insignificant loss of GY34 during the
26 453 centrifugal filtration.
27 453
28 454

29 455 **Effect of GY34 on organic osmolyte flux**

30 456 Cells exposed to physiological or cytotoxic stimuli are eliminated by apoptosis which is a genetically well-
31 457 orchestrated cellular process. Apoptosis is characterized by an initial cell shrinkage (apoptotic volume
32 458 decrease), which reflects net loss of ions, organic osmolytes and water.^{25,26} It has been shown that onset of
33 459 apoptosis can be postponed/prevented by limitation of the activity of volume-sensitive and volume-insensitive
34 460 leak pathways, that normally facilitate loss of the organic osmolyte taurine, and/or up-regulation of Na⁺-
35 461 dependent transporters, e.g. TauT that facilitates taurine accumulation.²⁷ Taurine accounts for about 0.1 % of
36 462 our total body weight²⁸ and besides being an important organic osmolyte in mammalian cells taurine is
37 463 recognized for its role in foetal development, lung function, mitochondrial function, antioxidative defense and
38 464 as a modulator of the apoptotic response once it has been initiated.²⁷ Cisplatin resistance in ELA cells, when
39 465 compared to Cisplatin-sensitivity in EATCs, has previously been demonstrated to correlate with less nuclear
40 466 Cisplatin accumulation, decrease in the initial ion- and water loss as well as an increased TauT activity.⁶ In
41 467 A2780 cells acquirement of Cisplatin resistance correlates with up-regulation in TauT activity and a
42 468 concomitant down-regulation in volume-sensitive taurine leak pathway.²⁹ In congruence, TauT activity has
43 469 been shown to promote Cisplatin resistance in kidney cells³⁰ and multidrug resistance in colorectal cancer.³¹
44 470
45 470
46 470
47 470
48 470
49 470

50 471 In the present work Cisplatin-sensitive A2780 WT cells (wild type), Cisplatin-resistant A2780 RES cells (acquired,
51 472 extrinsic resistance) as well as Cisplatin-resistant ELA cells (innate, intrinsic resistance) were exposed to 5 μ M
52 473 Cisplatin or 5 μ M GY34 for 18 h. Taurine influx and taurine release under isotonic conditions were determined
53 474 by tracer technique. From Fig. 7 it is seen that 18 h Cisplatin exposure increases taurine uptake and
54 475 concomitantly reduces taurine release in A2780 WT cells. It has recently been shown that Cisplatin resistance in
55 476 A2780 RES cells correlates with an increased taurine accumulation, following an increased ability to accumulate
56 477 taurine and a concomitant impairment of a volume-sensitive taurine release pathway²⁹, i.e. the response to
57 477
58 477
59
60

1
2
3
4
5
6
7 478 Cisplatin seen in A2780 WT cells (Fig. 7) most probably reflects initiation of a resistance phenotype within 18 h
8 479 exposure to Cisplatin. In contrast, 18 h exposure to Cisplatin has no effect on taurine transport in A2780 RES or
9 480 ELA cells. GY34 on the other hand reduces taurine uptake in all three cell lines and stimulates taurine release in
10 481 the resistant cell lines. As down-regulation of taurine uptake and increase in taurine release following exposure
11 482 to GY34 could reflect that GY34 induces cell death in wild type as well as the Cisplatin-resistant cell lines, the
12 483 progression of cell death and apoptosis in ELA cells following exposure to Cisplatin and GY34 was analyzed.
13 484 Initiation of apoptosis by chemical drugs typically involves DNA-damage, activation of specific kinases
14 485 (ATM/ATR) which through phosphorylation/activation of the transcription factor p53 provokes synthesis of
15 486 pro-apoptotic proteins and subsequently activation of caspase 3.²⁹ Exposure of phosphatidylserine on the
16 487 surface of apoptotic cells is a clear signal of apoptotic progression and normally serves as a signal to phagocytic
17 488 cells to engulf/degrade the apoptotic cell.³² From Fig. 8, which illustrates FACS analysis of ELA cells following
18 489 exposure to 5 μ M GY34 or 5 μ M Cisplatin for 18 h it can be seen that GY34 initiates cell death (increase in
19 490 propidium iodide signaling) and apoptosis (increase in annexin-V staining). This may indicate that GY34 initiates
20 491 cell death partly by apoptosis in Cisplatin-resistant cells and that GY34 therefore may be able to overcome
21 492 Cisplatin resistance.
22 493

23 494 **Conclusion**

24 495 Interestingly, a potential of the novel Ru-based compound GY34 in overcoming Cisplatin resistance has been
25 496 found in the present work. A novel fractionation procedure has been presented, able to obtain clean nuclei,
26 497 mitochondria and cytosol for prediction of the intracellular metallo-drug distribution. Furthermore, the stability
27 498 and transformation of the analyte during experiments have been found to significantly influence the outcome
28 499 and the importance of monitoring these parameters has thus been demonstrated. As an alternate, more
29 500 diverse approach than commonly practiced, considering both chemical and biological aspects has been applied
30 501 in this work, the experiments performed can be used as a general protocol and an additional tool in the initial
31 502 evaluation of novel metal-based drugs.
32 503

33 504 **Acknowledgements**

34 505 The authors kindly wish to thank Dorthe Nielsen who contributed significantly to the experimental work of this
35 506 paper and Camilla Jensen for assistance in the laboratory. We also thank COST1105 for facilitating the
36 507 collaboration between the Danish and Spanish contributors to this work. The work was supported by Faculty of
37 508 Health and Medical Sciences of University of Copenhagen, "Læge Sofus Carl Emil Friis og Olga Doris Friis's
38 509 legat", "Agnes og Poul Friis's Fond", the Spanish Ministerio de Economía y Competitividad and FEDER (Project
39 510 SAF2011-26611).
40 511

41 512 **References**

- 42 513 1. World Health Organization, <http://www.who.int/mediacentre/factsheets/fs297/en/>, (accessed January
43 514 2015)
44 515
- 45 516 2. S. Dasari, P.B. Tchounwou, *Eur. J. Pharmacol.*, 2014, **740**, 364-378
46 517
47 518
48 519
49 520
50 521
51 522

- 1
2
3
4
5
6
7 517
8
9 518 3. L. Galuzzi, L. Senovilla, I. Vitale, J. Martins, O. Kepp, M. Castedo, G. Kroemer, *Oncogene*, 2012, **31**, 1869-1883
10 519
11 520 4. C.A. Rabik, M.E. Dolan, *Cancer Treat. Rev.*, 2007, **33**, 9-23
12 521
13 522 5. G.S. Yellol, A. Donaire, J.G. Yellol, V. Vasylyeva, C. Janiak, J. Ruiz, *Chem. Comm.*, 2013, **49**, 11533-11535
14 523
15 524 6. H.S. Tastesen, J.B. Holm, J. Møller, K.A. Poulsen, C. Møller, S. Stürup, E.K. Hoffmann, I.H. Lambert, *Cell.*
16 525 *Physiol. Biochem.*, 2010, **26**, 809-820
17 526
18 527 7. L.H. Møller, C.S. Jensen, T.T.T.N. Nguyen, S. Stürup, B. Gammelgaard, *J. Anal. At. Spectrom.*, 2015, **30**, 277-
19 528 284
20 529
21 530 8. J.B. Holm, R. Grygorczyk, I.H. Lambert, *Am. J. Physiol. Cell Physiol.*, 2013, **305**, C48-C60,
22 531 DOI: 10.1152/ajpcell.00412.2012
23 532
24 533 9. K.R. Villumsen, L. Duelund, I.H. Lambert, *Amino Acids*, 2010, **39**, 1521-1536
25 534
26 535 10. D. Wang, S.J. Lippard, *Nat. Rev. Drug Discovery*, 2005, **4**, 307-320
27 536
28 537 11. Prof. José Ruiz, Department of Inorganic Chemistry, University of Murcia
29 538
30 539 12. V. Cepeda, M.A. Fuertes, J. Castilla, C. Alonso, C. Quevo, J.M. Pérez, *Anti-cancer Agents Med. Chem.*, 2010,
31 540 **10**, 3-18
32 541
33 542 13. E.E. Rojo, B. Guiard, W. Neupert, R.A. Stuart, *J. Biol. Chem.*, 1998, **273**, 8040-8047
34 543
35 544 14. H. Hornig-Do, G. Günther, M. Bust, P. Lehnartz, A. Bosio, R.J. Wiesner, *Anal. Biochem.*, 2009, **389**, 1-5
36 545
37 546 15. M.R. Wieckowski, C. Giorgi, M. Lebedzinska, J. Duszynski, P. Pinton, *Nat. Protoc.*, 2009, **4(11)**, 1582-1590
38 547
39 548 16. Z. Dai, J. Yin, H. He, W. Li, C. Hou, X. Qian, N. Mao, L. Pan, *Proteomics.*, 2010, **10**, 3789-3799
40 549
41 550 17. A. Zayed, T. Shoeb, S.E. Taylor, G.D.D. Jones, A.L. Thomas, J.P. Wood, H.J. Reid, B.L. Sharp, *Int. J. Mass*
42 551 *Spectrom.*, 2011, **307**, 70-78
43 552
44 553 18. M. Groessl, O. Zava, P.J. Dyson, *Metallomics*, 2011, **3**, 591-599
45 554
46 555 19. Thermo Fisher Scientific Inc., <http://www.piercenet.com/instructions/2161477.pdf>, (accessed January
47 556 2015)
48
49
50
51
52
53
54
55
56
57
58
59
60

- 1
2
3
4
5
6
7 557
8
9 558 20. Sigma-Aldrich Co., <https://www.sigmaaldrich.com/content/dam/sigmaaldrich/docs/Sigma/Bulletin/mitoiso2bul.pdf>, (accessed January 2015)
10 559
11 560
12 561 21. A. de Almeida, B.L. Oliveira, J.D.G. Correia, G. Soveral, A. Casini, *Coord. Chem. Rev.*, 2013, **257**, 2689-2704
13
14
15 562 22. A. Casini, J. Reedijk, *Chem. Sci.*, 2012, **3**, 3135-3144
16
17 563 23. Y. Kasherman, S. Stürup, D. Gibson, *J. Med. Chem.*, 2009, **52**, 4319-4328
18 564
19 565 24. P. Heffeter, K. Böck, B. Atil, M.A.R. Hoda, W. Körner, C. Bartel U. Jungwirth, B.K. Keppler, M. Micksche, W.
20 566 Berger, G. Koellensperger, *J. Biol. Inorg. Chem.*, 2010, **15**, 737-748
21
22 567
23 568 25. E.K. Hoffmann, I.H. Lambert, S.F. Pedersen, *Physiol. Rev.*, 2009, **89**, 193-277
24 569
25
26 570 26. I.H. Lambert, E.K. Hoffmann, S.F. Pedersen, *Acta Physiol. Scand.*, 2008, **194**, 255-282
27 571
28 572 27. I.H. Lambert, D.M. Kristensen, J.B. Holm, O.H. Mortensen, *Acta Physiol. (Oxf.)*, 2015, **213**, 191-212
29
30 573
31 574 28. R.J. Huxtable, *Physiol. Rev.*, 1992, **72**, 101-163
32 575
33
34 576 29. B. H. Sorensen, U. A. Thorsteinsdottir, I. H. Lambert, *Am. J. Physiol. Cell. Physiol.*, 2014, **307**, C1071-1080,
35 577 DOI: 10.1152/ajpcell.00274.2014
36 578
37 579 30. X. Han, J. Yue, R.W. Chesney, *J. Am. Soc. Nephrol.*, 2009, **20**, 1323-1332
38 580
39 581 31. M. Yasunaga, Y. Matsumura, *Sci. Rep.*, 2014, **4**, no. 4852, DOI: 10.1038/srep04852
40
41
42 582 32. J.G. Kay, S. Grinstein, in *Lipid-mediated Protein Signaling*, ed. D.G.S. Caputello, Springer Science, 2013, ch.
43 583 10, p. 177-193
44
45 584
46 585
47
48
49
50
51
52
53
54
55
56
57
58
59
60

1
2
3
4
5
6
7 586
8 587
9
10
11
12
13
14
15
16 593
17 594
18 595
19 596
20 596
21 597
22
23
24
25
26
27
28
29
30
31
32
33
34
35
36
37
38
39
40
41
42
43
44
45
46
47
48
49
50
51
52
53
54
55
56
57
58
59
60

Fraction	% GY34 in fraction	
	1	2
Nuclei	4	3
Mitochondria	18	21
Cytosol	78	76
	592	

Table 1: Intracellular distribution of GY34 in murine Ehrlich Lettré Ascites cells after 18 h incubation with nominally 10 μ M GY34. Values correspond to % GY34 found in each fraction out of the total GY34 found in nuclei, mitochondria and cytosol for two replicates.

1
2
3
4
5
6
7
8
9
10
11
12
13
14
15
16
17
18
19
20
21
22
23
24
25
26
27
28
29
30
31
32
33
34
35
36
37
38
39
40
41
42
43
44
45
46
47
48
49
50
51
52
53
54
55
56
57
58
59
60

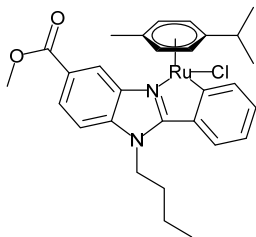


Figure 1: Structure of GY34⁹

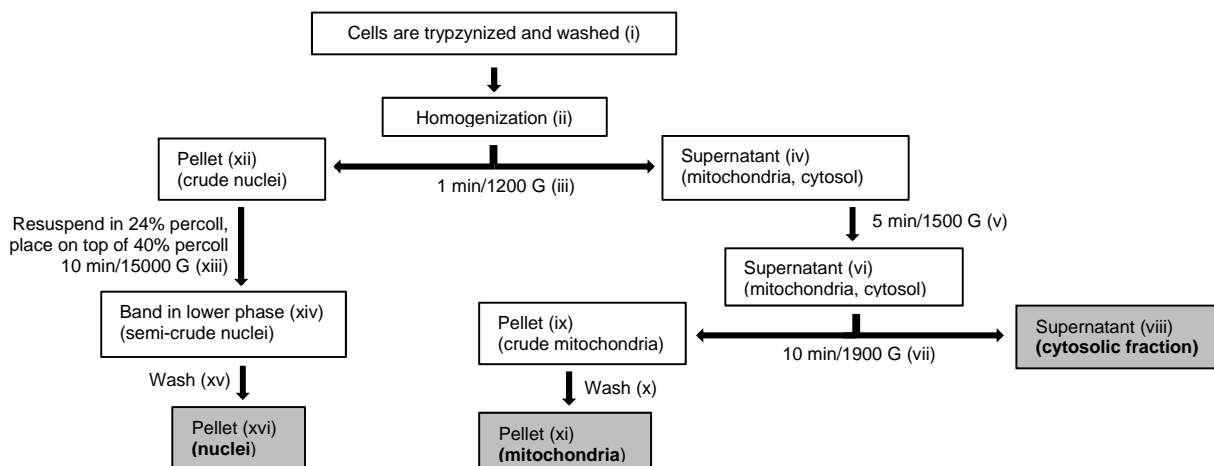


Figure 2: Overview of procedure used to fractionate murine Ehrlich Lettré Ascites cells into nuclei, mitochondria and cytosol. Roman numerals in parentheses refer to various steps in the process and are further specified in the experimental section Cell Fractionation.

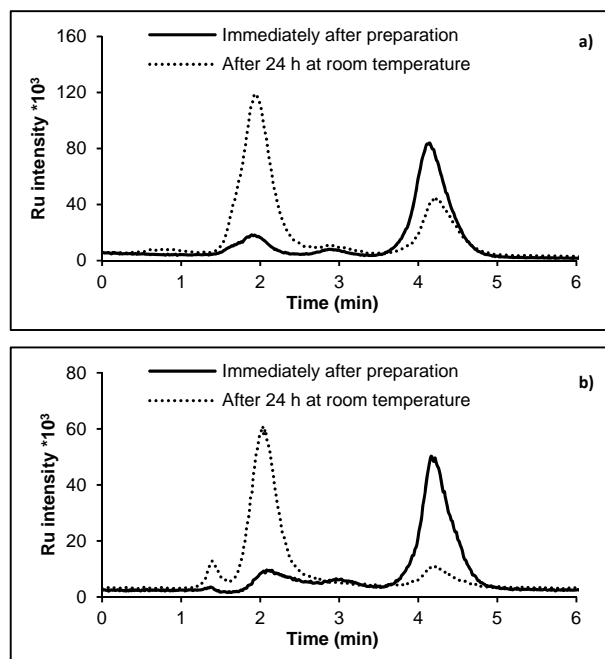
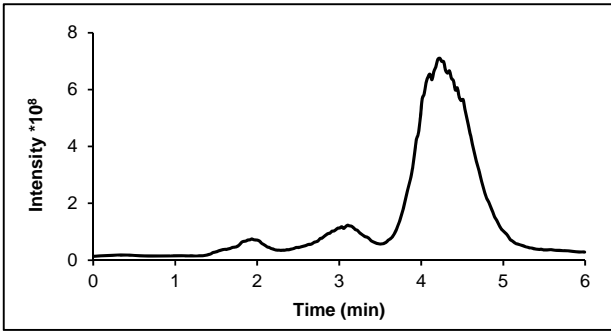


Figure 3: RP-HPLC-ICP-MS chromatograms of 1 μ M GY34 solutions in **a)** mobile phase (20 mM ammonium acetate in 65 % MeOH, pH 6.8) and **b)** RPMI-1640 cell medium. Solid curves were obtained immediately after preparation of the GY34 solutions and dotted curves after 24 h at room temperature.

1
2
3
4
5
6
7
8
9
10
11
12
13
14
15
16
17
18
19
20
21
22
23
24
25
26
27
28
29
30
31
32
33
34
35
36
37
38
39
40
41
42
43
44
45
46
47
48
49
50
51
52
53
54
55
56
57
58
59
60



613

Figure 4: Total ion chromatogram obtained from RP-HPLC-ESI-MS analysis of 1 mM GY34 in RPMI-1640 cell medium 24 h after preparation.

616

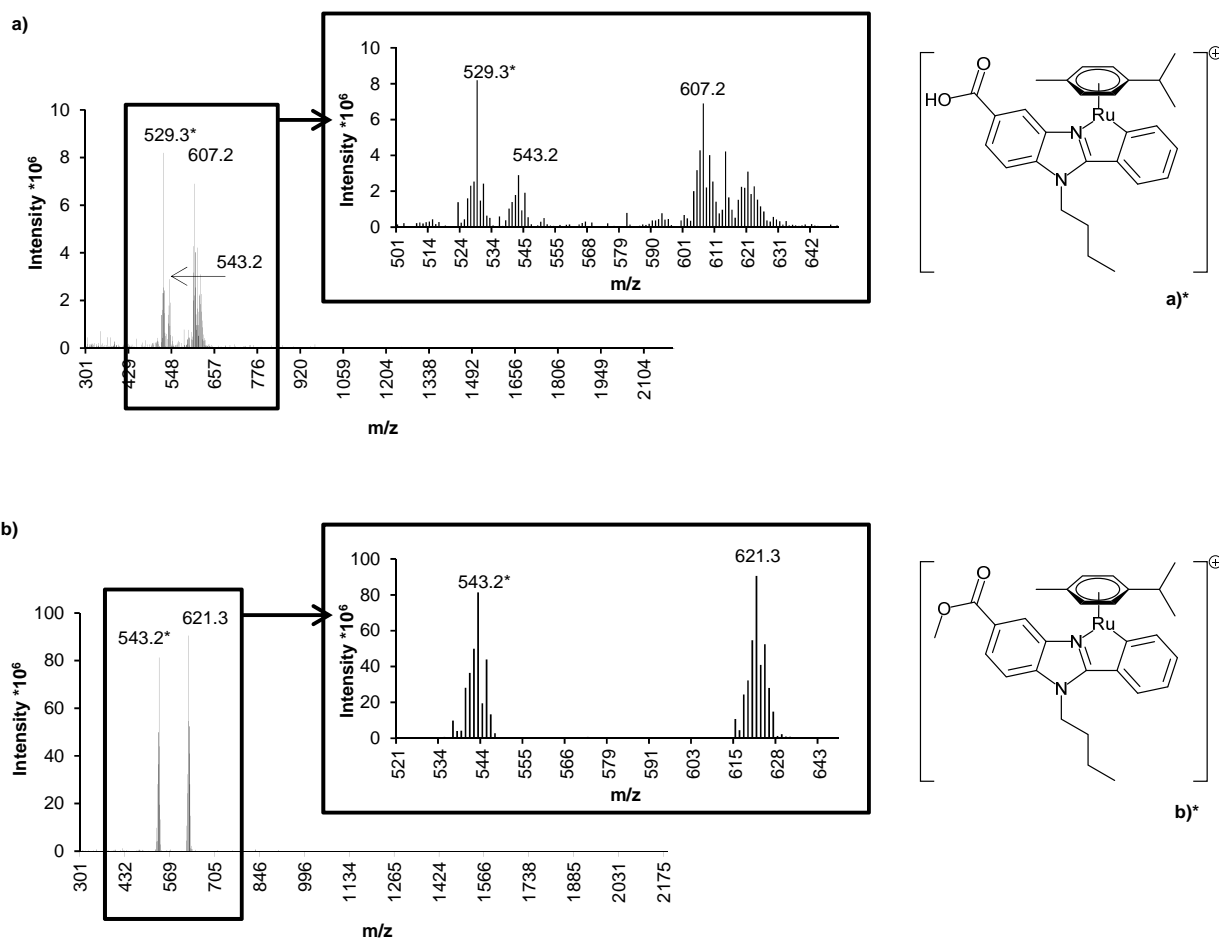


Figure 5: Mass spectra of **a)** the ~3 min and **b)** the ~4.5 min total ion chromatogram peaks in Fig. 4 with peaks of interest extracted. Structures of the m/z 529.3 and 543.2 species are depicted as **a)*** and **b)***, respectively.

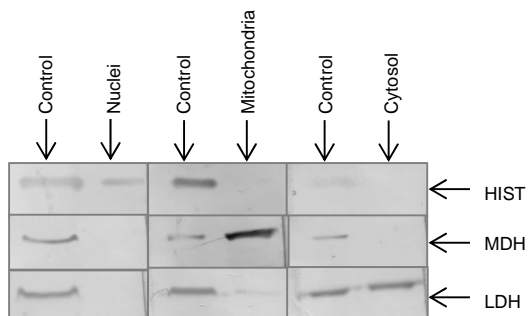


Figure 6: Representative western blot of nuclei, mitochondria and cytosol obtained from fractionation of murine Ehrlich Lettré Ascites cells incubated 18 h with nominally 10 μ M GY34 (n = 3). The left band of each membrane piece is the control (total cell homogenate) and the right band is the sample, *i.e.* nuclei, mitochondria or cytosol as indicated. The histone H3 (HIST, 18 kDa, marker for nuclei), malate dehydrogenase 2 (MDH, 36 kDa, marker for mitochondria) and lactate dehydrogenase B (LDH, 35 kDa, marker for cytosol) bands are indicated as well.

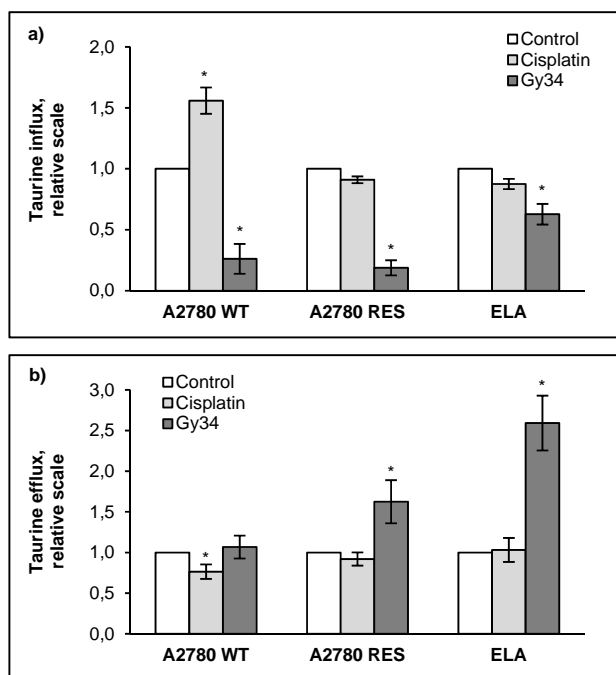


Figure 7: Taurine influx and taurine release under isotonic conditions in Cisplatin-sensitive wild type (A2780 WT) and acquired Cisplatin-resistant (A2780 RES) human ovarian carcinoma cells along with innate Cisplatin-resistant murine Ehrlich Lettré Ascites (ELA) cells. Cells were grown in the absence (white bars) or presence of either 5 μ M Cisplatin (light grey bars) or 5 μ M GY34 (dark grey bars) for 18 h before determination of taurine influx and taurine release by tracer technique as indicated in the experimental section Taurine Flux Assays. **a)** Influx is given relative to control values, *i.e.* 0.009 ± 0.001 (A2780 WT), 0.018 ± 0.002 (A2780 RES) and 0.157 ± 0.016 (ELA) $\text{nmol}\cdot\text{g}\cdot\text{prot}^{-1}\cdot\text{min}^{-1}$ and represent 8/3 (A2780 WT), 3/3 (A2780 RES) and 5/5 (ELA) sets of experiments with Cisplatin/GY34. **b)** Efflux, determined as the fractional rate constant, is given relative to control values, *i.e.*, 0.0044 ± 0.0003 (A2780 WT), 0.0028 ± 0.003 (A2780 RES) and 0.0022 ± 0.0003 (ELA) min^{-1} and represent 8/7 (A2780 WT), 8/6 (A2780 RES) and 9/5 (ELA) sets of experiments with Cisplatin/GY34. Values are given as mean values \pm SEM. *indicates significant difference from control values (Students t-test).

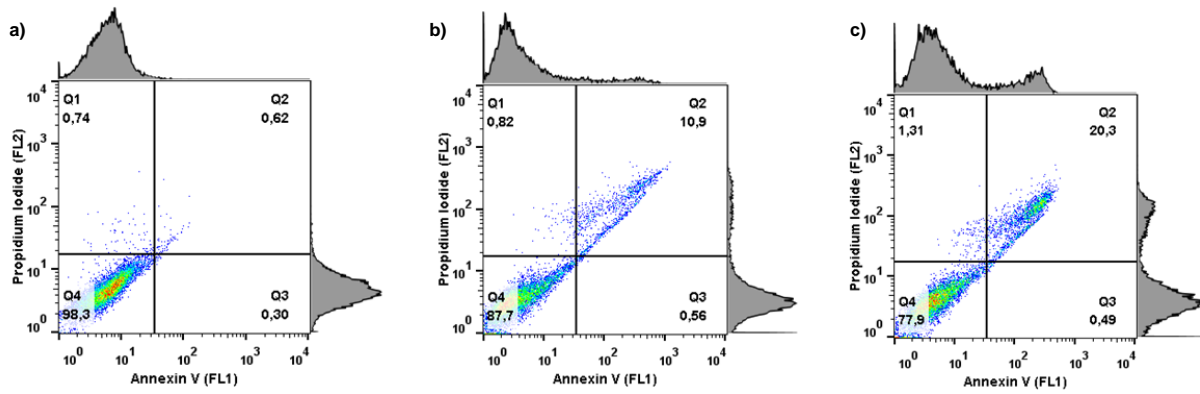
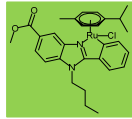


Figure 8: Representative FACS analysis dotplots of **a)** control (untreated murine Ehrlich Lettré Ascites (ELA) cells). **b)** ELA cells exposed to 5 μM Cisplatin for 18 h. **c)** ELA cells exposed to 5 μM GY34 for 18 h (n = 3). Migration to quadrant Q2 indicates apoptosis.

1
2
3
4
5
6
7
8
9
10
11
12
13
14
15
16
17
18
19
20
21
22
23
24
25
26
27
28
29
30
31
32
33
34
35
36
37
38
39
40
41
42
43
44
45
46
47
48
49
50
51
52
53
54
55
56
57
58
59
60

Novel metal-based drug



- Stability?
- Intracellular distribution?
- Cytosolic biomolecule binding?
- Osmolyte homeostasis?
- Apoptosis?

Applying a novel protocol for characterization of metal-based drugs reveals potential of a new Ru-based compound in overcoming Cisplatin resistance.